THE JOURNAL OF BIOLOGICAL CHEMISTRY VOL. 283, NO. 24, pp. 16808–16817, June 13, 2008

The Reaction of α-Synuclein with Tyrosinase
POSSIBLE IMPLICATIONS FOR PARKINSON DISEASE[*S]

Received for publication, November 2, 2007, and in revised form, March 26, 2008 Published, JBC Papers in Press, April 4, 2008, DOI 10.1074/jbc.M709014200

Isabella Tessari[‡], Marco Bisaglia[‡], Francesco Valle[§], Bruno Samorì[§], Elisabetta Bergantino[‡], Stefano Mammi[¶], and Luigi Bubacco[‡1]

From the Departments of [‡]Biology and [¶]Chemical Sciences, University of Padova, Padova 35121 and the [§]Department of Biochemistry, University of Bologna, Bologna 40126, Italy

Oxidative stress appears to be directly involved in the pathogenesis of Parkinson disease. Several different pathways have been identified for the production of oxidative stress conditions in nigral dopaminergic neurons, including a pathological accumulation of cytosolic dopamine with the subsequent production of toxic reactive oxygen species or the formation of highly reactive quinone species. On these premises, tyrosinase, a key copper enzyme known for its role in the synthesis of melanin in skin and hair, has been proposed to take part in the oxidative chemistry related to Parkinson disease. A study is herein presented of the *in vitro* reactivity of tyrosinase with α-synuclein, aimed at defining the molecular basis of their synergistic toxic effect. The results presented here indicate that, in conformity with the stringent specificity of tyrosinase, the exposed tyrosine sidechains are the reactive centers of α-synuclein. The reactivity of α-synuclein depends on whether it is free or membrane bound, and the chemical modifications on the tyrosinase-treated α-synuclein strongly influence its aggregation properties. On the basis of our results, we propose a cytotoxic model which includes a possible new toxic role for α-synuclein exacerbated by its direct chemical modification by tyrosinase.

Parkinson disease (PD)[2] is the most common movement disorder and, after Alzheimer disease, the second most common neurodegenerative disorder affecting ~1–2% of people over 65 years. It is a progressive disease characterized by the inability to initiate, execute, and control movements.

Neuropathologically, PD is characterized by a striking loss of dopamine-producing neurons in the substantia nigra pars compacta, accompanied by depletion of dopamine in the striatum, and by the presence of cytoplasmic inclusions known as Lewy bodies. Most forms of PD are sporadic, although, in some cases, familiar inheritance is observed. At present, at least 10 genetic loci have been associated to the disease (1). Although the etiopathogenesis of sporadic PD remains elusive, gene-related forms have provided some interesting evidence supporting a model of etiopathogenesis that involves mitochondrial dysfunction, increase of oxidative stress, ubiquitin-proteasome system deregulation, and protein misfolding and aggregation (2). Furthermore, because neurons in the substantia nigra pars compacta contain significant amounts of dopamine (DA), it has been proposed that DA itself or one of its metabolites, especially dopamine-quinones (DAQs), may account for the selective vulnerability of these neurons. DAQs are synthesized by oxidation of the catechol ring of DA (3); if this occurs within the neuronal cytosol, DAQs may react with cytosolic components and, specifically, with cysteine residues (4, 5). These residues are often part of the active site or play a pivotal role in function; as a consequence, covalent modifications of cysteine could lead to function impairment. DAQs have also been shown to increase mitochondrial damage and to inhibit the proteasome (6, 7). Among the cytoplasmic protein targets, DAQs have been found to react with α-synuclein (αSyn), a protein whose function is poorly understood, although its gene has been associated to familiar forms of PD (8).

αSyn is a small cytosolic protein of 14 kDa, largely expressed in neurons (9). It belongs to the natively unfolded protein family (10, 11), but it is also able to bind to membranes adopting a helical conformation (12). In agreement with the ability to interact with membranes, increasing evidence suggests that a possible key function of the protein is the modulation of synaptic vesicle recycling, which involves DA storage and release at nerve terminals by maintenance of a subset of presynaptic vesicles in the "reserve" pools (13–15). αSyn represents the main component of Lewy bodies, where it is found in a β-sheet-rich fibrillar form.

When the amount of cytosolic DA exceeds the physiological concentration, DA can be metabolized via monoamine oxidase and aldehyde dehydrogenase into the non-toxic metabolite 3,4-dihydroxyphenylacetic acid and hydrogen peroxide (16), or it can be sequestered into the lysosomes (17) where it can autooxidize to form neuromelanin (NM). NM is a stable polymer responsible for the dark pigmentation of the substantia nigra and is composed of indole, catechol, and benzothiazine rings, also containing lipids, iron, and quinone-like radicals. It has been suggested that NM formation itself may be neuroprotective because of both its scavenging activity toward toxic DAQs and the sequestering of metal ions, including iron, copper, manganese, and cadmium (17–20). Nevertheless, the dying neurons in PD have been observed to release NM in the cyto-

* This work was supported by the Progetti di Rilevante Interesse Nazionale and the Fondo per gli Investimenti della Ricerca di Base. The costs of publication of this article were defrayed in part by the payment of page charges. This article must therefore be hereby marked "*advertisement*" in accordance with 18 U.S.C. Section 1734 solely to indicate this fact.

[S] The on-line version of this article (available at http://www.jbc.org) contains supplemental Figs. S1 and S2.

[1] To whom correspondence should be addressed: Tel.: 39-049-827-6346; Fax: 39-049-827-6300; E-mail: luigi.bubacco@unipd.it.

[2] The abbreviations used are: PD, Parkinson disease; AFM, atomic force microscopy; αSyn, α-synuclein; DA, dopamine; DAQ, dopamine-quinone; NM, neuromelanin; SUV, small unilamellar vesicle; Ty, tyrosinase; *wt*, wild type; Tricine, *N*-[2-hydroxy-1,1-bis(hydroxymethyl)ethyl]glycine.

plasm and in the extracellular space, which results in the loss of the protective role of NM and, on the contrary, in the worsening of neurodegeneration (21).

The process of NM formation is still debated, and there is no a general agreement on the fact that it derives simply from non-enzymatic oxidative chemistry. The auto-oxidation of catechols to quinones with the subsequent addition of thiol groups has been demonstrated in the brain (22). Alternative enzymatic pathways have been suggested for NM synthesis, including tyrosine hydroxylase (23), peroxidase (24), prostaglandin H synthase (25, 26), xanthine oxidase (27), lipoxygenase (28), and monoamine oxidase (29). The enzyme tyrosinase (Ty), which is responsible for melanin synthesis within the melanosomes, has also been suggested to take part in the biosynthesis of NM. This suggestion was based on the observations that Ty mRNA was found in human substantia nigra (30) and that the Ty promoter is active throughout murine brain development, particularly in the substantia nigra of adult brain (31). In a previous work, we demonstrated that Ty is expressed in the human brain (32). We found that the mRNA coding for Ty and a detectable protein expression and enzymatic activity are present, although at low levels. Furthermore, in cell culture systems, expression of Ty increases neuronal susceptibility to oxidizing conditions, including dopamine itself.

In agreement with our results, another group, using neuronal cell lines that constitutively express αSyn and tetracycline-regulated Ty, demonstrated that co-expression of human αSyn with Ty significantly exacerbated cell death and was associated with the formation of αSyn oligomers induced by quinone derivatives (33).

With the purpose of better characterizing the interplay between Ty and αSyn, which can lead to enhanced oxidative conditions, we decided to focus our attention on the structural modifications that may be induced on αSyn by its reaction with Ty.

EXPERIMENTAL PROCEDURES

Protein Preparation and Purification—Human αSyn cDNA was amplified by PCR with synthetic oligonucleotides (Sigma-Genosys) containing NcoI and XhoI restriction sites and designed to obtain the entire sequence of the protein (αSyn140) or the region coding for the first 99 amino acids (αSyn99). After digestion with restriction enzymes, the two PCR products were subcloned into the NcoI-XhoI-linearized pET28b expression plasmid (Novagen) and introduced into an *Escherichia coli* BL21(DE3) strain. Overexpression of proteins was achieved by growing cells in LB medium (1% Bacto tryptone, 0.5% yeast extract, 0.5% NaCl) at 37 °C to an A_{600} of 0.6 followed by induction with 0.5 mM isopropyl β-thiogalactopyranoside for 4 h. After boiling the cell homogenate for 15 min, the soluble fraction, containing αSyn140 or αSyn99, was loaded into a Resource Q or Resource S 6-ml column (Amersham Biosciences), respectively, and then eluted using a NaCl gradient. When working with αSyn140, the eluted fractions containing the protein were further purified with a size-exclusion Superdex 200 column (Amersham Biosciences). Finally, the proteins were dialyzed against water, lyophilized, and stored at −20 °C. *Streptomyces antibioticus* tyrosinase was expressed and purified in our laboratory according to published procedures (34).

Reaction Mixtures—The samples used in all the spectroscopic analyses contained αSyn140 or αSyn99 to a final concentration of 100 μM in the presence of 100 mM phosphate buffer (pH 7.4) and with the addition of the indicated quantity of *S. antibioticus* tyrosinase.

Preparation of Small Unilamellar Vesicles—About 8 mg of a mixture of 50% dimyristoylphosphatidylcholine and 50% dimyristoylphosphatidylglycerol were used for the preparation of SUVs. In a typical preparation, the lipids were dissolved in 1 ml of chloroform/methanol (4:1), and the solution was evaporated under a nitrogen stream in a glass test tube. The dry lipid film was suspended in 100 mM phosphate buffer (pH 7.4) to give a stock solution with a final concentration of 30 mM and mixed for 1 h above the melting temperature. The hydration product was filtered through a large pore size (0.45 μm) filter and subsequently extruded at least 11 times through a 50 nm pore filter, following the manufacturer's protocol (Avanti Lipids).

Limited Proteolysis of αSyn99 by Chymotrypsin—A limited proteolysis experiment of αSyn99 in the presence of high purity chymotrypsin (Calbiochem) was carried out at 25 °C for 10 min in a reaction mixture containing 50 μg of protein and 1.5 units of chymotrypsin in 5–50 mM phosphate buffer (pH 7.4). The reaction was terminated by immediate boiling. The chymotryptic cleavage products of αSyn99 were analyzed by 15–20% gradient Tricine SDS-PAGE, containing 6 M urea, and stained by Coomassie R-250.

Nitro Blue Tetrazolium/Glycinate Redox-cycling Staining—Quinoproteins and related compounds were detected by redox-cycling staining (35). Briefly, the protein samples, separated by SDS-PAGE, were transferred to nitrocellulose membranes at 50 V for 90 min at 4 °C. Bound quinonoids were detected by immersing the membrane in a solution of 0.24 mM nitro blue tetrazolium, 2 M potassium glycinate (pH 10.0) for 45 min in the dark resulting in a bluish purple stain of quinoprotein bands and no staining of other proteins. After washing with 0.1 M borate buffer, pH 10.0, unmodified proteins were stained with Ponceau S (0.1% in 5% acetic acid) resulting in a red stain, whereas the already stained quinoproteins remained bluish purple.

UV-visible Spectroscopy and Kinetic Studies—Spectra were recorded on a diode-array Agilent 8453 UV-visible spectrophotometer interfaced with a personal computer using the Chemstation Software for Windows®. Optical measurement were performed at 25 °C using HELLMA quartz cells with Suprasil® windows and an optical path length of 1 cm. Spectra were recorded every 30 s for the first 5 min; then the time between successive spectra was progressively increased by 25% at every measurement up to 4 h. The wavelength range was of 190–1100 nm.

Fluorescence Experiments—Fluorescence emission spectra were recorded on a PerkinElmer Life Sciences LS 50 spectrofluorometer equipped with a thermostatted cell compartment and interfaced with a personal computer using the FL-WinLab program for Windows®. Sample measurements were carried out using a HELLMA ultra-micro cell with Suprasil® windows and an optical path length of 10 × 2 mm. Fluorescence spectra were

obtained at 25 °C, using excitation and emission wavelengths of 275 and 305 nm, respectively, with excitation bandwidth of 10 nm and emission bandwidth of 8 nm for αSyn140 and 13 nm for αSyn99. Excitation and emission spectra were recorded between 250 and 295 nm and 285 and 340 nm, respectively, at a scan rate of 100 nm/min.

NMR Experiments—Spectra were recorded on a Bruker Avance DMX600 spectrometer equipped with a gradient triple resonance probe. Samples were prepared as described above, but the protein was dissolved in 99.9% D_2O. Clean-total correlation spectroscopy spectra were recorded in the phase-sensitive manner using the TPPI method (36, 37) with a 100-ms mixing time. The experiments were carried out by collecting 128 increments, each one consisting of 32 scans and 2048 data points. The spectral width was 1796 Hz (^{1}H-direct) and 6000 Hz (^{1}H-indirect). The frequency offsets were 4500 Hz (^{1}H-direct) and 2323.8 Hz (^{1}H-indirect) The time domain data were multiplied by a 90° shifted sin function in all dimensions before Fourier transformation.

Pseudo two-dimensional experiments were obtained by acquiring a series of 16 one-dimensional experiments, each one consisting of 512 scans and 8192 data points. The spectral width was 7183.9 Hz, and the frequency offset was 2824.8 Hz.

CD Experiments—CD measurements were carried out on a JASCO J-715 spectropolarimeter interfaced with a PC. The CD spectra were acquired and processed using the J-700 program for Windows®. All experiments were carried out at room temperature using HELLMA quartz cells with Suprasil® windows and an optical path length of 0.1 cm. All spectra were recorded in the 190–260 nm wavelength range, using a bandwidth of 2 nm and a time constant of 2 s at a scan speed of 50 nm/min. The signal-to-noise ratio was improved by accumulating at least four scans. All spectra are reported in terms of mean residue molar ellipticity $[\Theta]_R$ (deg cm^2 dmol^{-1}).

Amyloid Fibril Formation—A 500-μl aliquot of αSyn140 (150 μM) was first incubated with Ty (in 100 mM phosphate buffer, pH 7.4, with a molar ratio Ty/αSyn = 1/1000) at 25 °C for 4 h and then maintained at 37 °C with continuous shaking for the time span reported in the figures. An equal aliquot of αSyn140 without Ty was incubated under the same experimental conditions for comparison. The same procedure was used for a 150 μM aliquot of the N-terminal fragment αSyn99.

AFM Imaging—Every 24 h, a 10-μl aliquot was collected from each experimental solution and blotted onto a freshly cleaved mica surface. Further dilutions (10–10,000 times) were occasionally performed to tune a good sample dispersion on the substrate surface. The droplet was allowed to dry, and then the sample was thoroughly rinsed with milliQ water and blown dry with a nitrogen flux.

Images of these samples were recorded using a Multimode AFM (Veeco Metrology Inc., Santa Barbara, CA) operated in tapping mode under ambient conditions. The cantilevers employed were Pointprobes (Nanosensors, Neuchatel, Switzerland) with a nominal tip radius of curvature of <10 nm and a resonance frequency between 310 and 370 kHz.

Images were analyzed using the free software WSxM (Nanotec Electronica) (38). The size of the particles was measured using the section analysis tool, and it was estimated from their height relative to the surface, because this parameter is not influenced by the tip convolution effect.

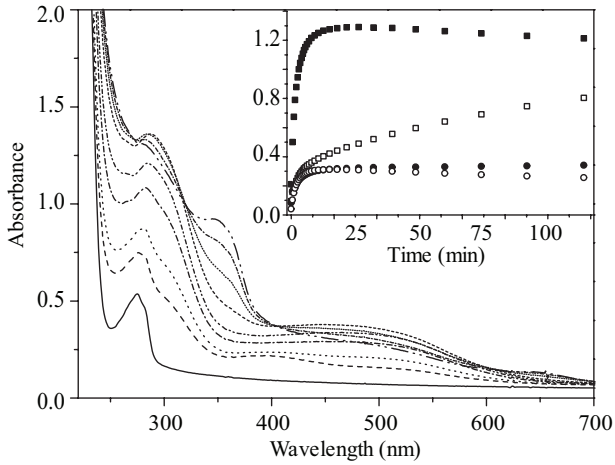

FIGURE 1. **UV-visible spectral changes associated to the reactions between Ty and αSyn.** The selected spectra of αSyn140 were recorded at 0 (*solid line*), 1 (– – –), 1.5 (·····), 3 (– · – ·), 5 (– · · – ·), 20 (-----), 60 (·····), 120(-·-·-), and 180 (— · ·) min after the addition of Ty. The *inset* represents the time dependence of the variation in absorbance at the wavelengths indicated below, which correspond the most important spectral features (see supplemental materials). *Filled squares* = 294 nm, *open squares* = 354 nm, *filled circles* = 400 nm, and *open circles* = 490 nm.

RESULTS

α-Synuclein as a Substrate for Tyrosinase—The unfolded state of αSyn in solution and the presence of four tyrosine residues in the sequence suggest the possibility that these residues may act as substrates for the monooxygenase and dioxygenase activity of Ty leading to quinones. The time evolution of the reaction was monitored by recording a series of UV-visible spectra of wild type (*wt*) αSyn in the presence of Ty in a molar ratio of 1000:1. The results are shown in Fig. 1 (see also supplemental Fig. S1*A*). The spectrum of αSyn140 before the reaction was subtracted from the spectra collected during the time course of the reaction. The time dependence of the spectral changes in Fig. 1, *inset panel*, shows at least four peaks with different absorbance maxima and characterized by different kinetic parameters. The time dependence of the optical spectra reveals first the decrease of the peak at ~280 nm assigned to the starting tyrosine and phenylalanine, partially masked by the raising 294 nm feature. The first reaction product can only be observed as a broad feature at 400 nm in the first two spectra recorded within the first minute of reaction. This absorption band is compatible with the formation of the quinone by tyrosinase (3) that first acts as monooxygenase and then converts the diphenol to quinone. The second product generated is characterized by the two features, the first more intense at 294 and the second at 490 nm. These absorption bands are tentatively associated to the formation of aminochrome (3). The last observable product is associated to the increase in absorbance observed at 354 nm that becomes observable after the 294 and 490 nm features begin to decrease. The key aspect of these results is that the observed reactivity appears to be strongly related to the unfolded state of αSyn, and it is independent on the sequence, because all four tyrosine residues seem to be reactive as will be discussed later in the NMR experiments. Further-

more, by using the protein bovine serum albumin as substrate, in a control experiment, no modification in the UV-visible spectrum was observed (data not shown). It is worth noting that bovine serum albumin has 21 tyrosine residues that, according to the crystal structure of human serum albumin (where 19 of these tyrosine are fully conserved), are all buried in the hydrophobic core of the protein.

To unravel the complex reaction of *wt* αSyn with Ty, we chose to simplify the system by working with the deletion mutant αSyn99. This fragment contains only one tyrosine at position 39 and lacks the three other tyrosine residues (Tyr-125, Tyr-133, and Tyr-136) of the *wt* protein. In the presence of αSyn99 and Ty in a molar ratio of 1000:1, we observed similar spectroscopic features to those observed for the *wt* αSyn. The main differences are that the first quinone (400 nm) is probably too low in concentration to be detectable (supplemental Fig. S1*B*), and the absence of the 650 nm feature that is likely to derive from downstream reactions not feasible in the presence of only one tyrosine residue. As a control, we also tested the reaction in a sample of αSyn without Ty: no reaction was observed (data not shown) confirming that the spectral changes depend on the presence of Ty.

α-Synuclein Residues Involved in the Reaction with Tyrosinase—To confirm that tyrosine residues really represent the substrates for Ty, we followed the changes in the fluorescence spectrum of αSyn140 and αSyn99 in the presence of Ty using the excitation (276 nm) and emission (305 nm) wavelengths characteristic of the tyrosine residue. During the time span of the experiment, the peak intensities progressively decreased (Fig. 2); this is compatible with the formation of non-fluorescent species, such as quinones. It is worth noting that the rate of decrease in fluorescence intensity is quite different for the *wt* protein and the αSyn99 fragment.

A further indication of the involvement of tyrosine residues and of the formation of quinone species was obtained by combining a chymotrypsin proteolysis (known to be selective for aromatic residues) and a quinone-specific staining. The complex cleavage pattern expected for αSyn140 before and after the treatment with Ty prompted us to carry out these experiments on the smaller αSyn99 fragment. The expected cleavage pattern for αSyn99 is presented in Table 1. If the tyrosine residue at position 39 is modified by Ty, no recognition by protease can take place, and the cleavage pattern should be modified with respect to the untreated αSyn. The results of the SDS-PAGE separation of untreated and treated samples are shown in Fig. 3*A*. In the untreated sample (*lanes 1* and *2*), after digestion of αSyn99 with chymotrypsin (*lanes 2*), a new band appears corresponding to the expected fragment of 55 residues (αSyn40–94). The fragment of 35 residues is not visible on the gel most likely because of its small size. The sample treated with Ty (*lanes 3* and *4*) was not cleaved by chymotrypsin at position 39, and the only band that appears in the gel corresponds to αSyn99 protein cleaved at positions 4 and 94, αSyn5–94 (*lane 4*). It is worth noting that, after Ty treatment, modified αSyn99 also forms a small fraction of dimeric species. In Fig. 3*B*, the results obtained after transferring the samples to nitrocellulose and staining them with a quinoprotein-specific dye (35) are shown. Although the untreated αSyn99 is stained only by Ponceau red,

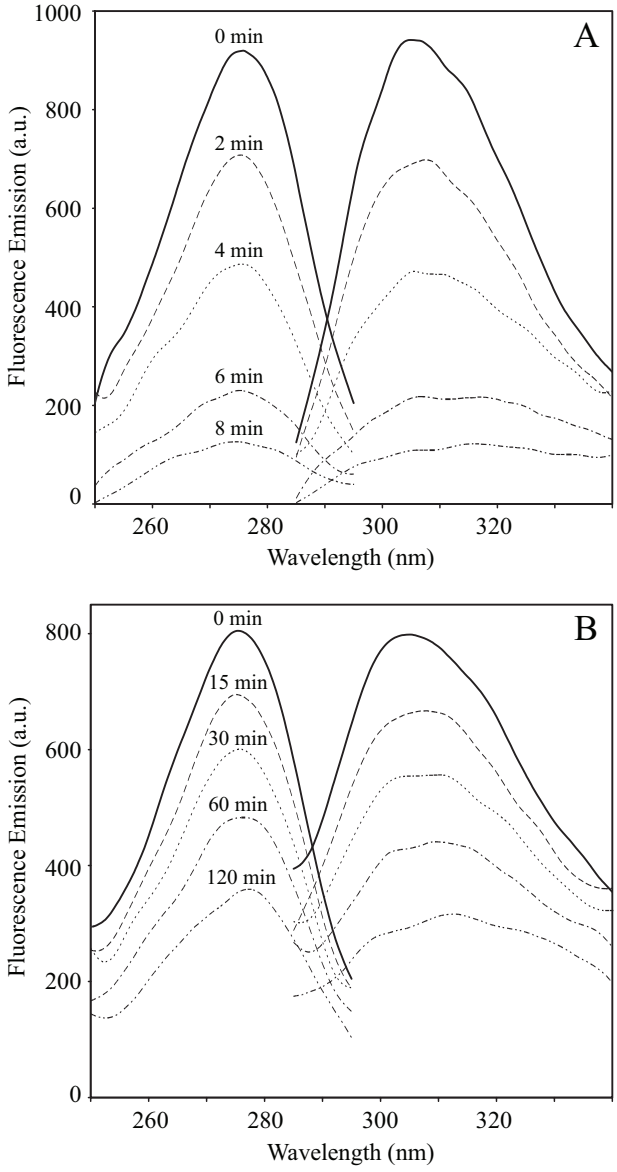

FIGURE 2. **Tyrosine involvement in the reaction between Ty and αSyn.** Fluorescence spectra of αSyn140 (*A*) and αSyn99 (*B*), excitation spectra on the *left* and emission spectra on the *right*, were recorded using emission and excitation wavelengths of 305 and 275 nm, respectively. After the addition of Ty, the fluorescence intensity progressively decreases during the evolution of the reaction, showing that tyrosine is the substrate of the enzyme.

αSyn99 treated with Ty becomes bluish purple, indicating the formation of tyrosine-derived quinones.

The time evolution of the reaction products was analyzed by NMR spectroscopy. The experiments were carried out in D_2O to simplify the analysis of the aromatic region of the spectrum. First, we assigned the peaks corresponding to the aromatic amino acids of αSyn by means of total correlation spectroscopy experiments (data not shown). Then, pseudo-two-dimensional NMR spectra of the reactions between αSyn140 or αSyn99 and Ty, in a substrate to enzyme molar ratio of 1000:1, were recorded for 4 h. The results obtained in the presence of the *wt* protein are shown in Fig. 4. After the addition of Ty, the intensities of the peaks corresponding to tyrosine residues were strongly reduced in agreement with the previously described decrease of the 282 nm absorbance peak. The fact that the reac-

TABLE 1
Proteolytic pattern of chymotrypsin against αSyn99

Sites of proteolytic cleavage	Fragment sequence	Fragment length	Molecular mass
			Da
4	MDVF	4	510.6
39	MKGLSKAKEGVVAAAEKTKQGVAEAAGKTKEGVLY	35	3549.1
94	VGSKTKEGVVHGVATVAEKTKEQVTNVGGAVVTGVTAVAQKTVEGAGSIAAATGF	55	5268.9
99	VKKDQ	5	616.7

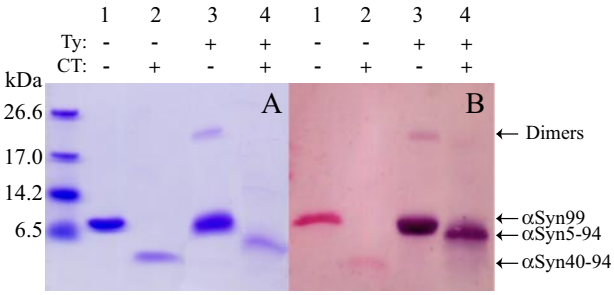

FIGURE 3. **Quinone formation observed on αSyn99 following the incubation with Ty.** αSyn99 samples were subjected to a highly specific proteolytic cleavage and analyzed by either SDS-PAGE (*A*) or Western blotting (*B*). *Lanes 1* and *2* correspond to αSyn99 before and after the cleavage reaction in the presence of chymotrypsin, respectively. *Lanes 3* and *4* are similar to the previous ones, but αSyn99 was previously treated with Ty. The absence of the expected cleavage pattern, and the appearance of the typical quinoprotein coloration on αSyn99 treated with Ty, strongly suggests the involvement of tyrosine in the formation of quinone species.

tion stopped a few minutes after the addition of the enzyme is probably due to the consumption of the oxygen dissolved in solution, which is necessary for Ty. Also the peaks corresponding to histidine 50, the only histidine present in the protein, disappeared indicating that this residue is somehow involved in a later stage of the reaction that may not involve tyrosinase. A possible reaction is represented by the nucleophilic attack of the imidazole ring of the histidine to a quinone ring of the modified tyrosines. Finally, in the spectra recorded after the addition of Ty, some degree of peak broadening can be observed with a general loss of resolution. This is probably due to the formation of dimeric species, most probably dityrosine or histidine-tyrosine cross-linked species. It is worth noting that the integration value of the phenylalanine peaks remains comparable before and after the addition of Ty. This observation confirms the specificity of the reaction observed and indicates that the decreased intensity of the tyrosine signals is not due to the relaxation effects of radicals potentially formed in solution. The results obtained with the fragment αSyn99 are in strong agreement with the previous ones, although the reaction with Ty was slower, as previously observed in our fluorescence experiments. As shown in Fig. 5, after ~2 h tyrosine peaks completely disappeared while four new peaks in the region of 5.5–6.7 ppm appeared soon after the beginning of the reaction. These peaks, which are also present in the NMR spectrum of the *wt* protein (data not shown), have a low intensity and can be associated to the late products observed by optical spectroscopy. A more detailed analysis of the 6.7–7.9 ppm spectral region showed that the peaks corresponding to histidine 50 diminished ~30% in intensity during the evolution of the reaction.

Effects of the Reaction with Tyrosinase on αSyn-membrane Interaction—CD spectroscopy was used to define whether Ty-induced modifications on αSyn could affect the propensity of

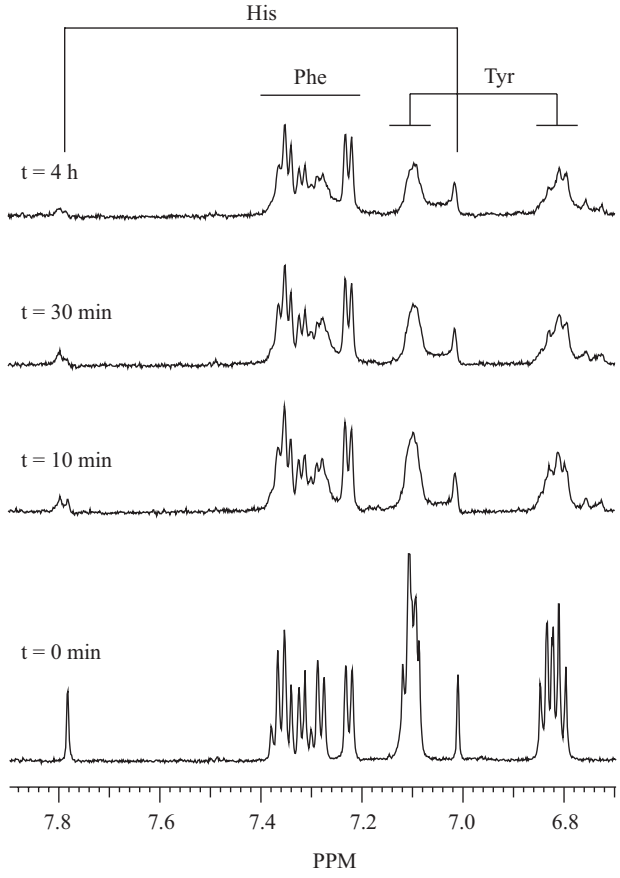

FIGURE 4. **Structural characterization of the reaction between αSyn140 and Ty.** The one-dimensional ^{1}H NMR spectra were recorded in deuterated water to make only the non-exchangeable protons of αSyn visible in the aromatic region of the spectra. The aromatic amino acid side chains corresponding to the peaks visible in the spectra are indicated. After the addition of Ty, peaks corresponding to tyrosine residues and to histidine 50 rapidly disappear.

the protein to fold and interact with membranes. The four tyrosines of αSyn cluster in two groups. The single N-terminal Tyr-39 resides within the lipid binding domain of the protein, whereas the C-terminal tyrosines are located in the flexible and well accessible C-terminal tail. For this reason, we carried out our analyses both on the full-length protein and the αSyn99 fragment, by comparing the spectra recorded before and after the reaction with Ty, in the absence and in the presence of SUV. In agreement with our previous results (39, 40), we chose to work with a lipid to protein molar ratio of 200 to maximize the binding of αSyn to the membrane.

The spectra shown in Fig. 6*A* indicate that modifications induced by Ty considerably perturb the ability of αSyn140 to interact with vesicles. On the contrary, modified αSyn99 retains most of its ability to bind to membranes, as shown in Fig. 6*B*. This fragment undergoes a conformational transition to a

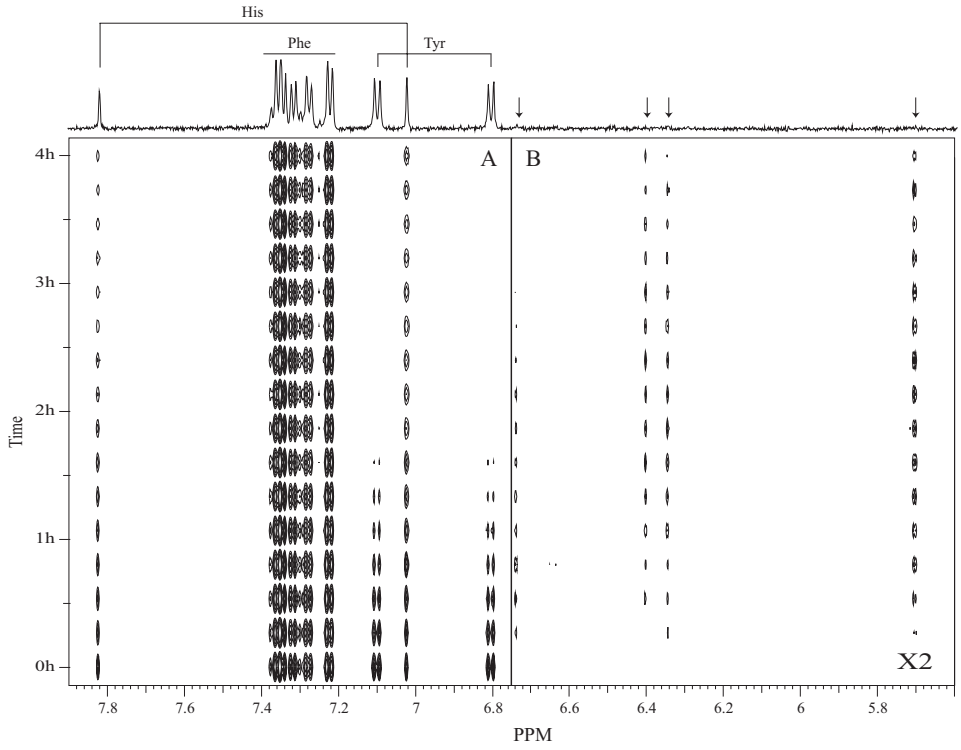

FIGURE 5. **Structural characterization of the reaction between αSyn99 and Ty.** Pseudo two-dimensional NMR spectrum of αSyn99 recorded in deuterated water after the addition of Ty. The aromatic amino acid side chains corresponding to the peaks visible in the spectra are indicated. The *horizontal axis* is extended to 5.6 ppm to show the appearance of new peaks during the evolution of the reaction, indicated by *arrows*. The intensities of the signals in *panel A* are half those of the signals in *panel B*, to permit a better visualization of the disappearance of the peaks corresponding to histidine 50 that accompanies the loss of the peaks corresponding to tyrosine 39.

helical state independent of the time progression of the reaction, and the differences in the molar ellipticity values of the control αSyn99 and of the samples at the two time points investigated are small. This result indicates that, contrary to what is observed for αSyn140, modifications of αSyn99 residues alter the binding equilibrium between protein and vesicles only to a minor extent. A way to rationalize this different behavior comes from the comparison of the SDS-PAGE separations of both proteins before and after treatment with Ty (supplemental Fig. S2). As already indicated in Fig. 3, Ty-treated αSyn99 forms only a small fraction of dimeric species, and the intensity of the band corresponding to the monomer is very similar to that present in the control. After treatment of the αSyn140 sample with Ty, the band relative to the monomer is less intense and several new bands corresponding to oligomeric species appear.

Effects of α-Synuclein-Membrane Interaction on the Reaction with Tyrosinase—In parallel with the experiment described above, UV-visible spectroscopy was used to verify the dependence of the reaction with Ty on the folded state of αSyn. First, the evolution of the reaction between αSyn140 and Ty was monitored, in the same experimental conditions described above. The analysis was complicated by the light scattering caused by the presence of the vesicles in solution. Nevertheless, the region between 300 and 750 nm was still detectable. As reported in Fig. 7*A*, the increased absorbance at 490 nm suggests that the reactivity of Ty is not inhibited by the presence of SUV, and the results were comparable to those obtained without SUV, considering that three of the four tyrosine residues are free to react with Ty even if the modified chemical environment may lead to different reactivities. The results obtained by working in the presence of αSyn99 are different, and a very low reactivity was observed, with a lag phase that lasted for more than 1 h after the addition of Ty (Fig. 7*B*). These results suggest that, when αSyn99 is bound to the vesicles, the only tyrosine present (Tyr-39) is protected by the membrane and confirm the hypothesis that the Ty reactivity depends on tyrosine exposure. The residual reactivity observed might be originated by the presence of a small fraction of unbound αSyn99, in agreement with the presence of an equilibrium between free and SUV-bound protein, as previously described (41).

CD spectroscopy was used to analyze the effects of Ty incubation on the conformational properties of membrane-bound αSyn140 or αSyn99. In agreement with the very low reactivity observed in the UV-visible experiments, the conformation of αSyn99 did not change after the incubation period in the presence of Ty (Fig. 7*D*). The CD spectrum of αSyn140 presents only minor differences (Fig. 7*C*) despite the reactivity observed that likely involves only the tyrosine residues in the unstructured C-terminal region.

Effects of the Reaction with Tyrosinase on α-Synuclein Fibril Formation—AFM was used to quantify the capability of the Ty-modified αSyn to form fibrils. The control experiment is presented in Fig. 8 (*A* and *B*), where the starting monomeric αSyn140 is shown (Fig. 8*A*) together with the well characterized fibrils formed after 444 h of incubation at 37 °C (Fig. 8*B*). The picture obtained after 444 h of incubation of αSyn140 treated with Ty, under the same conditions of the control sample, is shown in *panel C*: no fiber could be observed in the image. The Ty treatment, however, affects the morphology of the sample, as the comparison of *panel A* and *panel C* reveals. To quantify this difference, the distribution of heights for the features in the images (the most reliable measure in AFM) of the two samples was compared (*panel D*). The distribution of heights for the monomeric, untreated αSyn140 is broad and centered at 3.5 nm, whereas the Ty-treated sample (centered at 6.5 nm) shows a narrow distribution of values that has to be fitted with an additional shoulder on the lower side of the Gaussian. This almost monodisperse population of spherical objects is compatible, in terms of volume, with the small αSyn oligomeric aggregates described in the literature (42). It is also possible to observe an annular oligomer similar to those reported by Conway *et al.* (43).

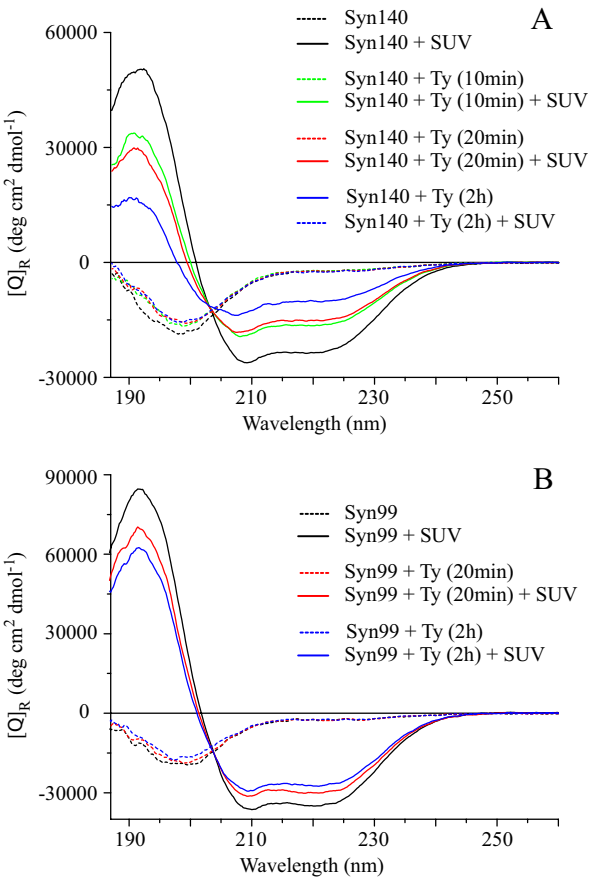

FIGURE 6. **Phospholipid-induced folding of untreated and treated αSyn.** The far-UV CD spectra of αSyn140 (*A*) and αSyn99 (*B*) in 100 mM sodium phosphate (pH 7.4), in the absence or in the presence of SUVs, are compared with the same spectra recorded at different times after the addition of Ty.

An analogous inhibition of the fibrillation process upon reaction with Ty was observed for the deletion mutant αSyn99 (data not shown). This result suggests that the modification of Tyr-39 by Ty may be sufficient to inhibit the formation of fibrils.

DISCUSSION

Oxidative stress has been proposed as one of the possible etiologic agents in PD (44, 45). In the literature, several different pathways have been identified for the oxidative stress induced by the oxidation of DA, including the production of toxic reactive oxygen species or the formation of highly reactive quinone species. On these premises, tyrosinase, a key copper enzyme known for its role in the synthesis of melanin in skin and hair, has been proposed to take part in the oxidative chemistry related to PD. Following this working hypothesis, in a previous work we demonstrated that Ty is ubiquitously expressed in the human brain, although at low levels, and its activity was found to be highest in the substantia nigra (32). It was also observed that expression of Ty in M17 cell lines increased neuronal susceptibility to αSyn toxicity. The latter result was later independently confirmed by other investigators (33). In this study, we present an *in vitro* characterization of the reactivity of Ty toward αSyn in the attempt to define the molecular basis of the synergistic toxic effect of Ty and αSyn.

The first result that emerges clearly from the data presented is that the observed reactivity is strongly a consequence of the unfolded conformation of αSyn in solution. The solvent-exposed tyrosine residues are the only substrates for both the monooxygenase and diphenol oxidase activity of Ty. The quinones generated by Ty on αSyn, however, are very reactive species and decrease in concentration to undetectable levels very early in the reaction. These quinones can react in several possible ways. The first one is the formation of a tyrosine dimer that can be either intramolecular or intermolecular. The intermolecular reaction is supported by the observation of dimer formation in the Ty-treated αSyn99 sample, which contains only one tyrosine residue. The strictly denaturant conditions used in the experiments for the detection of dimers support the formation of covalently bound dimers that, however, represent only a small fraction of the quinone positive species. This aspect seems to be particularly relevant and will be further discussed later, considering the literature data on dimeric, dityrosine cross-linked prenuclei that accumulate before the formation of fibrils and promote the fibrillation process of αSyn (46, 47). The second non-enzymatic reaction possible for the αSyn quinones is the cyclization to form a substituted leucoaminochrome that is then converted, in both enzymatic and non-enzymatic pathways, to aminochrome (48). The proposed reaction is consistent with the observed formation of a chromophore absorbing at both 294 and 490 nm that strongly resembles a similar aminochrome previously characterized among the dopamine oxidation products (3). An attempt was made to characterize the aminochrome quinone species by NMR, but the transient nature of this form only allowed the detection of low intensity peaks in the 5.7–6.8 ppm region of the NMR spectrum, compatible with the proposed product (3). The third non-enzymatic reaction possible for the αSyn quinones (including aminochrome) involves a histidine residue. The NMR results presented here indicate that His-50, the only histidine residue present in the protein, is another possible residue of αSyn that can be modified after the reaction of the protein with Ty. This is particularly evident in the case of *wt* αSyn. The simplest model, which takes our experimental observations into account, involves the nucleophilic attack of the imidazole ring of the histidine onto the quinone ring of the modified tyrosine, as previously described (49). However, this reaction does not fully justify the decreased intensity of the histidine peaks observed in our NMR spectra suggesting that other pathways may be also involved. In agreement with this conclusion, the last product detected, characterized by the absorption band centered at 354 nm, could not be identified suggesting that a complex series of reactions occurs downstream.

A second aspect analyzed in this work is the ability of the modified αSyn to interact with SUVs. Considering that the modified tyrosine residues are placed in regions that are not structured upon binding to SUVs, *i.e.* the loop between the two α-helices for Tyr-39 and the C-terminal region for the other three tyrosine residues, we could expect that incubation of αSyn in the presence of Ty did not change its ability to interact with membranes. Although this is true in the case of αSyn99, tyrosine modifications on αSyn140 inhibit the binding of the protein with SUV, probably by promoting cross-linking intra- and intermolecular reactions as suggested by the presence of oligomeric species in the SDS-PAGE separation. Interestingly,

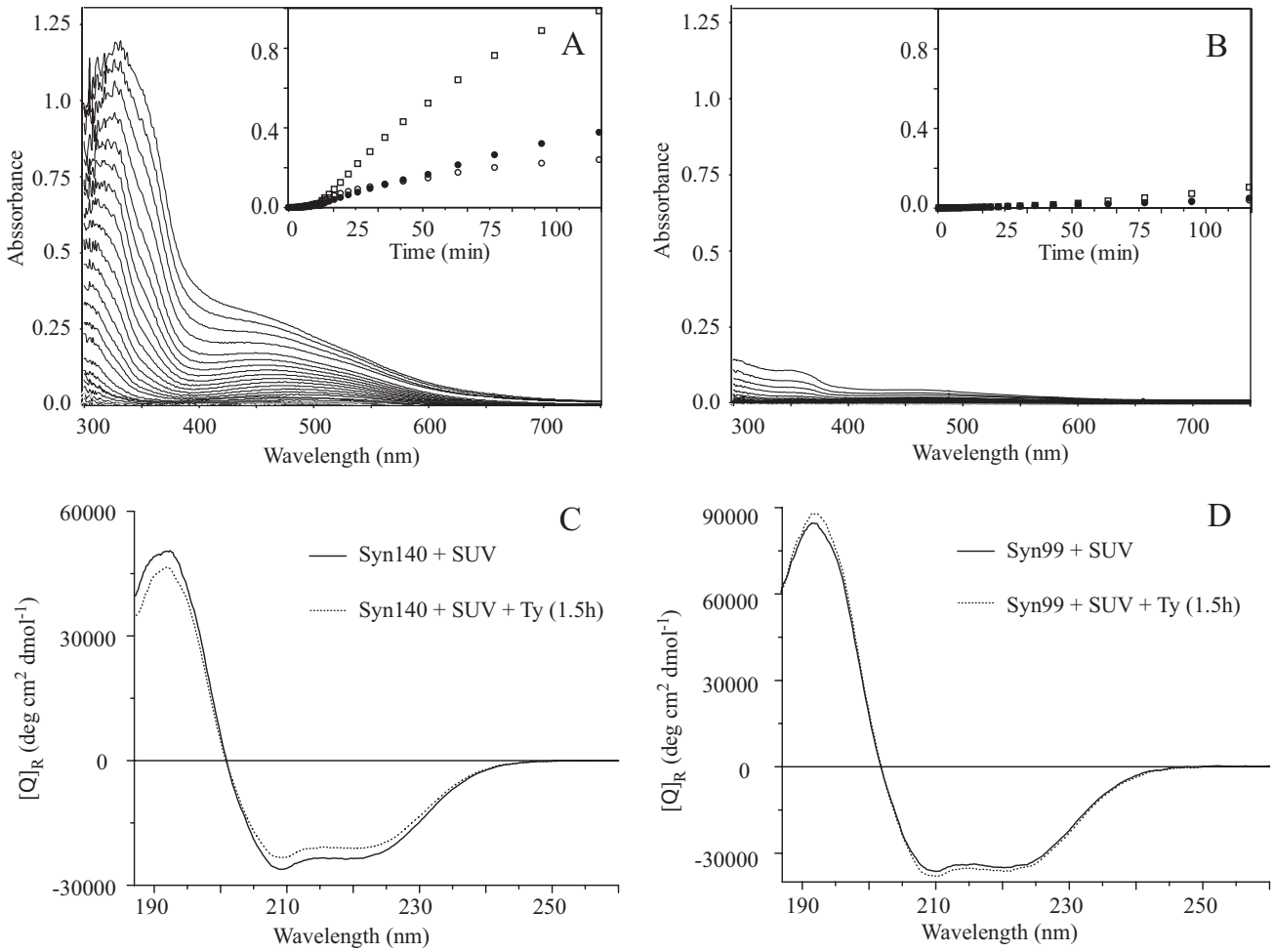

FIGURE 7. **Effects of αSyn/membrane interaction on the reactivity of Ty toward α-synuclein.** UV-visible spectra of αSyn140 (*A*) and αSyn99 (*B*) were recorded for 2 h in the presence of SUVs using a lipid to αSyn molar ratio of 200. The spectra reported were obtained by subtracting the αSyn spectrum before the reaction from the spectra recorded after Ty addition. Light scattering induced by the presence of SUV is responsible for a loss of resolved signal below 350 nm. The *inset* represents the time dependence of the variation in absorbance at the wavelengths indicated below, which correspond to the most important spectral features (see supplemental). *Open squares* = 354 nm, *filled circles* = 400 nm, and *open circles* = 490 nm. Far-UV CD spectra of membrane-bound αSyn140 (*C*) and αSyn99 (*D*) before and after 1.5 h of incubation in the presence of Ty.

when the reaction was carried out on the membrane-bound αSyn140, the modifications induced on the C-terminal tyrosines did not drastically alter the membrane interaction properties of the protein.

Therefore, in the membrane-bound state of αSyn, the residues involved in subsequent reactions with the C-terminal-modified tyrosines are protected. The helical fold induced on αSyn by the presence of vesicles also protects Tyr-39, as demonstrated by the observation that αSyn99 is not modified by Ty in these conditions. The lack of reactivity is not due to a direct inhibitory effect of the membrane on Ty, because the C-terminal tyrosine residues of *wt* αSyn are converted to quinones. The observed protection effect of a more physiological membrane-mimetic environment (SUV) is in agreement with our previous finding based on NMR experiments, in which Tyr-39 was reported to penetrate into SDS micelles (39). The present results do not support other topological models present in the literature in which Tyr-39 is on the hydrophilic side of the helix (50–52) or possibly at the membrane-water interface (53).

The definition of the possible reactions between αSyn and Ty is complicated by the presence, *in vivo*, of other substrates of Ty, such as dopamine. The data reported here must be framed within a complete description of the neurodegeneration process. A cytotoxicity model which involves αSyn and Ty must also include the oxidative stress generated by other reactive species, which may contribute to the progression of PD. The physiological role of Ty is to catalyze the conversion of imported DA and other catechols into NM within the lysosomes. Actually, lysosomes are thought to be involved in the uptake of excess cytoplasmic DA, which would otherwise undergo oxidation (17). Under pathological conditions, in which an excess of αSyn can be produced and/or when the lysosome content is released into the cytoplasm, Ty can react with αSyn, inducing local modifications that may hinder physiological functions of the protein. As the functions of αSyn seem to be related to DA metabolism and storage, hindering of these functions may induce a toxic process that leads to increased levels of cytosolic DA with consequent neuronal damage.

The actual mechanism of cellular toxicity associated to the formation of the various αSyn quinones is a central issue. The competence of neuronal cells to degrade this modified αSyn, either through the proteasome or the lysosome/autophagy

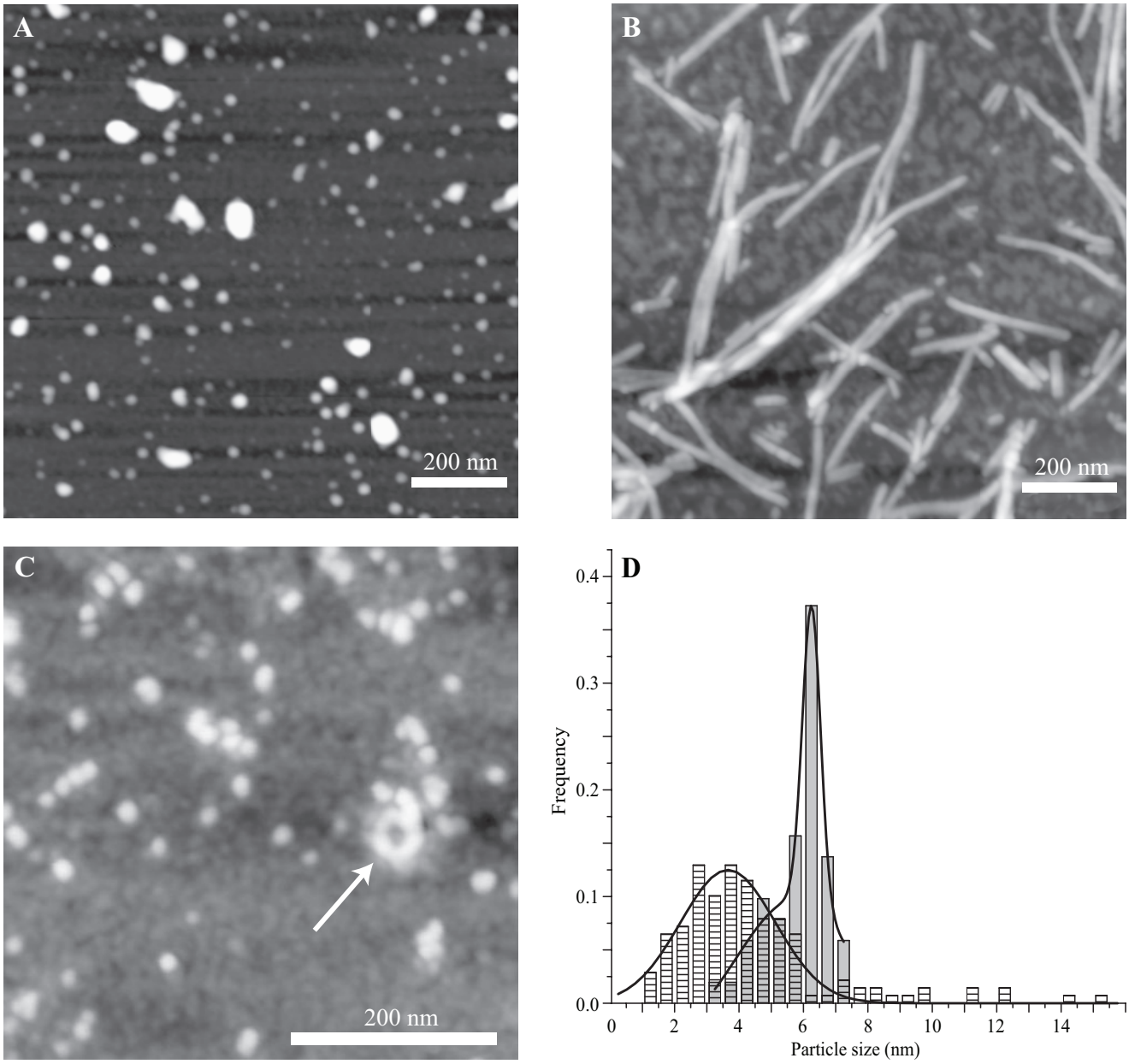

FIGURE 8. **Aggregation properties of tyrosine-modified α-synuclein.** *A*, αSyn140, control sample before incubation at 37 °C. *B*, αSyn140 fibers obtained upon incubation of the solution at 37 °C for 444 h. *C*, sample treated with tyrosinase in solution for 4 h and then deposited after the same incubation time: no fibers are present on the entire sample surface. An annular oligomer is indicated by the *arrow*. *D*, histograms of the heights of the particles present in a region of 1 μm × 1 μm; frequencies were defined as the number of events normalized to 1. The *grid columns* represent the population before incubation at 37 °C, whereas the *gray columns* are relative to the Ty-treated sample after 444 h of incubation at 37 °C under continuous shaking. The *black lines* are Gaussian fits of the main peaks present in each distribution.

pathway, starts to be defined now. Recently, Martinez-Vicente *et al.* (54) reported that dopamine-modified αSyn is poorly degraded by chaperone-mediated autophagy, but also blocks degradation of other substrates by this pathway. The αSyn/DAQs adducts may pose the same constraints as the A30P αSyn mutant to the activity of the chaperone-mediated autophagy leading to toxic gains of function (55) and more in general to the accumulation of these oxidized αSyn products.

The aggregation properties of the Ty-treated αSyn lead to a possible mechanism for the synergistic effect observed. The almost complete inhibition of fibril formation observed suggests that the toxic action may be linked to the oligomerization process that has been repeatedly invoked for several of the chemical modifications that occur for αSyn (56). The partial oxidation of some of the methionine residues, observed also in our experiments (data not shown), has been proven to be sufficient to hinder the fibrillation process (57) but not to give a complete inhibition as observed in the experiments presented here. In fact, we have shown that αSyn treated with Ty appears to form small aggregates that are statistically larger than the starting material supporting the formation of an oligomeric species that may be the key to the toxic effect.

In conclusion, the results presented here provide the first experimental study of the Ty reactivity toward αSyn. The reac-

tivity of αSyn depends on whether it is free or membrane-bound, and the reaction products may act as the toxic agent in the cell as a consequence of their aggregation properties. The detailed chemical characterization of the modified αSyn derivatives provides the groundwork to embark on validating the proposed chemistry by detecting these reaction products *in vivo*.

REFERENCES

1. Hardy, J., Cai, H., Cookson, M. R., Gwinn-Hardy, K., and Singleton, A. (2006) *Ann. Neurol.* **60,** 389–398
2. Corti, O., Hampe, C., Darios, F., Ibanez, P., Ruberg, M., and Brice, A. (2005) *C. R. Biol.* **328,** 131–142
3. Bisaglia, M., Mammi, S., and Bubacco, L. (2007) *J. Biol. Chem.* **282,** 15597–15605
4. Ito, S., Kato, T., and Fujita, K. (1988) *Biochem. Pharmacol.* **37,** 1707–1710
5. LaVoie, M. J., Ostaszewski, B. L., Weihofen, A., Schlossmacher, M. G., and Selkoe, D. J. (2005) *Nat. Med.* **11,** 1214–1221
6. Berman, S. B., and Hastings, T. G. (1999) *J. Neurochem.* **73,** 1127–1137
7. Fornai, F., Lenzi, P., Gesi, M., Ferrucci, M., Lazzeri, G., Busceti, C. L., Ruffoli, R., Soldani, P., Ruggieri, S., Alessandri, M. G., and Paparelli, A. (2003) *J. Neurosci.* **23,** 8955–8966
8. Xu, J., Kao, S. Y., Lee, F. J., Song, W., Jin, L. W., and Yankner, B. A. (2002) *Nat. Med.* **8,** 600–606
9. Clayton, D. F., and George, J. M. (1998) *Trends Neurosci.* **21,** 249–254
10. Weinreb, P. H., Zhen, W., Poon, A. W., Conway, K. A., and Lansbury, P. T. (1996) *Biochemistry* **35,** 13709–13715
11. Uversky, V. N., Gillespie, J. R., and Fink, A. L. (2000) *Proteins* **41,** 415–427
12. Davidson, W. S., Jonas, A., Clayton, D. F., and George, J. M. (1998) *J. Biol. Chem.* **273,** 9443–9449
13. Murphy, D. D., Rueter, S. M., Trojanowski, J. Q., and Lee, V. M. (2000) *J. Neurosci.* **20,** 3214–3220
14. Cabin, D. E., Shimazu, K., Murphy, D., Cole, N. B., Gottschalk, W., McIlwain, K. L., Orrison, B., Chen, A., Ellis, C. E., Paylor, R., Lu, B., and Nussbaum, R. L. (2002) *J. Neurosci.* **22,** 8797–8807
15. Lotharius, J., Barg, S., Wiekop, P., Lundberg, C., Raymon, H. K., and Brundin, P. (2002) *J. Biol. Chem.* **277,** 38884–38894
16. Elsworth, J. D., and Roth, R. H. (1997) *Exp. Neurol.* **144,** 4–9
17. Sulzer, D., and Zecca, L. (2000) *Neurotox. Res.* **1,** 181–195
18. Sulzer, D., Bogulavsky, J., Larsen, K. E., Behr, G., Karatekin, E., Kleinman, M. H., Turro, N., Krantz, D., Edwards, R. H., Greene, L. A., and Zecca, L. (2000) *Proc. Natl. Acad. Sci. U. S. A.* **97,** 11869–11874
19. Zecca, L., Zucca, F. A., Wilms, H., and Sulzer, D. (2003) *Trends Neurosci.* **26,** 578–580
20. Fedorow, H., Tribl, F., Halliday, G., Gerlach, M., Riederer, P., and Double, K. L. (2005) *Prog. Neurobiol.* **75,** 109–124
21. Zecca, L., Zucca, F. A., Albertini, A., Rizzio, E., and Fariello, R. G. (2006) *Neurology* **67,** S8–S11
22. Fornstedt, B., Rosengren, E., and Carlsson, A. (1986) *Neuropharmacology* **25,** 451–454
23. Haavik, J. (1997) *J. Neurochem.* **69,** 1720–1728
24. Okun, M. R. (1996) *Physiol. Chem. Phys. Med. NMR* **28,** 91–100
25. Mattammal, M. B., Strong, R., Lakshmi, V. M., Chung, H. D., and Stephenson, A. H. (1995) *J. Neurochem.* **64,** 1645–1654
26. Hastings, T. G. (1995) *J. Neurochem.* **64,** 919–924
27. Foppoli, C., Coccia, R., Cini, C., and Rosei, M. A. (1997) *Biochim. Biophys. Acta* **1334,** 200–206
28. Rosei, M. A., Blarzino, C., Foppoli, C., Mosca, L., and Coccia, R. (1994) *Biochem. Biophys. Res. Commun.* **200,** 344–350
29. Rabey, J. M., and Hefti, F. (1990) *J. Neural Transm. Park. Dis. Dement. Sect.* **2,** 1–14
30. Xu, Y., Stokes, A. H., Freeman, W. M., Kumer, S. C., Vogt, B. A., and Vrana, K. E. (1997) *Brain Res. Mol. Brain Res.* **45,** 159–162
31. Tief, K., Schmidt, A., and Beermann, F. (1998) *Brain Res. Mol. Brain Res.* **53,** 307–310
32. Greggio, E., Bergantino, E., Carter, D., Ahmad, R., Costin, G. E., Hearing, V. J., Clarimon, J., Singleton, A., Eerola, J., Hellstrom, O., Tienari, P. J., Miller, D. W., Beilina, A., Bubacco, L., and Cookson, M. R. (2005) *J. Neurochem.* **93,** 246–256
33. Hasegawa, T., Matsuzaki-Kobayashi, M., Takeda, A., Sugeno, N., Kikuchi, A., Furukawa, K., Perry, G., Smith, M. A., and Itoyama, Y. (2006) *FEBS Lett.* **580,** 2147–2152
34. Bubacco, L., Vijgenboom, E., Gobin, C., Tepper, A., Salgado, J., and Canters, G. W. (2000) *J. Mol. Catal. B-Enzym.* **8,** 27–35
35. Paz, M. A., Fluckiger, R., Boak, A., Kagan, H. M., and Gallop, P. M. (1991) *J. Biol. Chem.* **266,** 689–692
36. Bax, A., and Davis, D. G. (1985) *J. Magn. Res.* **65,** 355–360
37. Griesinger, C., Otting, G., Wütrich, K., and Ernst, R. R. (1988) *J. Am. Chem. Soc.* **110,** 7870–7872
38. Horcas, I., Fernández, R., Gomez-Rodriguez, J. M., Colchero, J., Gomez-Herrero, J., and Baro, A. M., *Rev. Sci. Instrum.* 78:013705, 2007
39. Bisaglia, M., Tessari, I., Pinato, L., Bellanda, M., Giraudo, S., Fasano, M., Bergantino, E., Bubacco, L., and Mammi, S. (2005) *Biochemistry* **44,** 329–339
40. Bisaglia, M., Schievano, E., Caporale, A., Peggion, E, and Mammi, S. (2006) *Biopolymers* **84,** 310–316
41. Bussell, R., Jr., and Eliezer, D. (2004) *Biochemistry* **43,** 4810–4818
42. Apetri, M. M., Maiti, N. C., Zagorski, M. G., Carey, P. R., and Anderson, V. E. (2006) *J. Mol. Biol.* **355,** 63–71
43. Conway, K. A., Lee, S. J., Rochet, J. C., Ding, T. T., Williamson, R. E., and Lansbury, P. T., Jr. (2000) *Proc. Natl. Acad. Sci. U. S. A.* **97,** 571–576
44. Hirsch, E. C. (1993) *Eur. Neurol.* **33,** 52–59
45. Jenner, P. (1998) *Mov. Disord.* **13,** 24–34
46. Souza, J. M., Giasson, B. I., Chen, Q., Lee, V. M., and Ischiropoulos, H. (2000) *J. Biol. Chem.* **275,** 18344–18349
47. Krishnan, S., Chi, E. Y., Wood, S. J., Kendrick, B. S., Li, C., Garzon-Rodriguez, W., Wypych, J., Randolph, T. W., Narhi, L. O., Biere, A. L., Citron, M., and Carpenter, J. F. (2003) *Biochemistry* **42,** 829–837
48. Kahn, V., and Ben-Shalom, N. (1998) *Pigment Cell. Res.* **11,** 24–33
49. Xu, R., Huang, X., Morgan, T. D., Prakash, O., Kramer, K. J., and Hawley, M. D. (1996) *Arch. Biochem. Biophys.* **329,** 56–64
50. Chandra, S., Chen, X., Rizo, J., Jahn, R., and Sudhof, T. C. (2003) *J. Biol. Chem.* **278,** 15313–15318
51. Bussell, R., Jr., and Eliezer, D. (2003) *J. Mol. Biol.* **329,** 763–778
52. Jao, C. C., Der-Sarkissian, A., Chen, J., and Langen, R. (2004) *Proc. Natl. Acad. Sci. U. S. A.* **101,** 8331–8336
53. Ulmer, T. S., Bax, A., Cole, N. B., and Nussbaum, R. L. (2005) *J. Biol. Chem.* **280,** 9595–9603
54. Martinez-Vicente, M., Talloczy, Z., Kaushik, S., Massey, A. C., Mazzulli, J., Mosharov, E. V., Hodara, R., Fredenburg, R., Wu, D. C., Follenzi, A., Dauer, W., Przedborski, S., Ischiropoulos, H., Lansbury, P. T., Sulzer, D., and Cuervo, A. M. (2008) *J. Clin. Invest.* **118,** 777–788
55. Cuervo, A. M., Stefanis, L., Fredenburg, R., Lansbury, P. T., and Sulzer, D. (2004) *Science* **305,** 1292–1295
56. Lashuel, H. A., and Lansbury, P. T., Jr. (2006) *Q Rev. Biophys.* **39,** 167–201
57. Glaser, C. B., Yamin, G., Uversky, V. N., and Fink, A. L. (2005) *Biochim. Biophys. Acta* **1703,** 157–169